Initial Stages of Interdiffusion of PMMA across an Interface

K. Kunz† and M. Stamm*

Max-Planck-Institut für Polymerforschung, Postfach 3148, 55021 Mainz, Germany

Received February 14, 1995; Revised Manuscript Received October 18, 1995⊗

ABSTRACT: The time dependence of the diffusion process at the interface between two thin films of protonated and deuterated poly(methyl methacrylate) (PMMA) is studied. By neutron reflection, we investigate both the form and the width of the interface between the two polymer layers with subnanometer resolution. At small diffusion times the movement of chain segments across the interface is followed in detail. Different characteristic time regimes for the broadening of the interface are distinguished. In addition, the form of the interfacial profile changes during the diffusion process and deviates at small diffusion times significantly from an error function profile, which would be assumed for normal Fickian diffusion. The results are discussed within the predictions of the reptation model and are compared to experiments with polystyrene films.

Introduction

The interdiffusion of polymers at an interface between two melt films is a process which influences many applications of polymers in practice, for instance melt processing or welding of blends. In order to understand the nature of polymer diffusion, a molecular description of the diffusion process is required. In the melt, polymer chains are entangled (if a certain molecular weight is exceeded) and cannot move freely.[1,2] This has its consequences on the broadening at the interface between two polymer melt films with time as well as on the form of the diffusion profile.[3,4] The study of initial stages of polymer diffusion at an interface can give information about the mechanism of the motion of a polymer chain in the melt. There have been several experimental investigations using the resolution of neutron reflectrometry[5−13] in the past few years. This includes mostly the investigation of the interdiffusion of polystyrenes,[5−9] but also different components with changing compatibilities and different mobilities have been used.[10−13] In this work, we investigate the initial stages of interdiffusion at the interface of poly(methyl methacrylate) (PMMA) melt films. The results are compared to theoretical predictions and to similar experiments with polystyrene, in order to determine whether a universal behavior can be found.

Polymer diffusion in the melt can be described within the framework of the reptation model by Edwards[1] and de Gennes.[2] In this model, the movement of a polymer chain is restricted to a tube formed by the entanglement network of the surrounding chains. Within this tube the chains move by a Rouse-type motion[14] along their contour. This results in a characteristic time behavior of the average displacement of the chain segments $\langle r^2\rangle^{1/2}$. At small diffusion times the average displacement of the chain segments is less than or equal to the radius of gyration of the molecule and deviations from classical Fickian diffusion are expected:[3,15] For very small times, smaller than the entanglement time τ_e, the segments still do not feel the constraints of the surrounding chains and $\langle r^2\rangle^{1/2} \sim t^{1/4}$. At τ_e the displacement is approximately given by the diameter of the tube. For $\tau_e \lesssim t \lesssim \tau_R$ the movement perpendicular to the tube is restricted by entanglements and $\langle r^2\rangle^{1/2} \sim t^{1/8}$. At the Rouse relaxation time τ_R the movement of the segments of the whole chain becomes correlated and $\langle r^2\rangle^{1/2} \sim t^{1/4}$ for $\tau_R \lesssim t \lesssim \tau_d$. For times longer than the reptation time $t \gtrsim \tau_d$ normal Fickian diffusion is expected with $\langle r^2\rangle^{1/2} \sim t^{1/2}$. It was the aim of several computer simulations[16−19] and experiments using neutron spin echo,[20−24] nuclear magnetic resonance,[25] and neutron reflectrometry[5−9] to learn details of this segmental diffusion process. While the two $t^{1/4}$ regimes have been confirmed in several investigations, the actual $t^{1/8}$ regime, which is characteristic for the reptation model, proves to be quite difficult to be resolved clearly.

The connectivity of the polymer molecules does not only affect the time behavior of the displacement of the polymer segments but has also its consequences on the form of the concentration profile at the interface.[4,26−28] According to the reptation picture, the movement of the whole chain can only proceed via the chain ends. If two polymer layers are brought into contact, initially no chains are crossing the interface. Therefore a discontinuity occurs, which decreases with annealing time and disappears at the reptation time τ_d. Since a movement of the chain segments within the tube is possible, this discontinuity is smeared out.[28] However, the profile is initially much steeper at the interface as compared to a normal diffusion profile. It is still further smeared out by surface roughness effects and capillary waves. For a more rigorous treatment of the time dependence of segmental motion at the interface, one would of course also have to take into account the distortion of chain conformations at the interface and the surface enrichment of ends. These influences are, however, difficult to treat theoretically and are only known from computer simulations of the free surface of a film (for a discussion see e.g. ref 29). One thus can only speculate on their importance for the interdiffusion process. In our experiments, however, one can clearly resolve different time regimes of interfacial broadening and a non-Gaussian concentration profile at initial stages of interdiffusion, as will be shown below.

Experimental Section

Sample Preparation. For the neutron reflectivity experiments relatively large bilayer samples (typically 10×10 cm^2) of protonated and deuterated PMMA films are prepared by spin coating and the floatation technique. Two different samples were used, which were subsequently annealed for

* To whom correspondence should be addressed.
† Present address: Foundation for Research and Technology−Hellas, Institute of Electronic Structure and Laser, P.O. Box 1527, 71110 Heraklion Crete, Greece.
⊗ Abstract published in *Advance ACS Abstracts,* February 15, 1996.

0024-9297/96/2229-2548$12.00/0

Table 1. Characteristic Data of the Polymers Used

polymer	M_w	M_w/M_n	T_g (°C)	iso/syndio (%)	supply
PMMA	85 500	1.05	120	5/38	PSS
PMMAd	82 000	1.08	121		PSS
PMMAd	85 100	1.06	122		PL

different times and quenched to room temperature for the neutron measurements. Characteristic data of the materials are given in Table 1. One sample (sample A) consisted of a protonated PMMA film (M_w = 85 500, thickness = 90 nm) on top of a deuterated PMMAd film (M_w = 82 000, thickness = 55 nm) on a float glass substrate. The other sample (sample B) had a deuterated PMMAd film (M_w = 85 100, thickness = 76 nm) on top of a deuterated PMMAd film (M_w = 85 500, thickness = 62 nm). The polymers used were purchased from Polymer Standards Service (PSS) and Polymer Laboratories (PL). They were characterized by gel permeation chromatography (GPC) and differential scanning calorimetry (DSC). For the GPC the PMMA was dissolved in tetrahydrofuran (THF) and PMMA standards were used for calibration. The DSC measurements were performed at a heating rate of 10 °C/min. The apparent values of T_g obtained from those heating runs are expected to be approximately 3 deg too high, since the averaged values from heating and cooling runs are typically 3 deg lower.[37] In addition, the tacticity of the protonated material was determined with proton NMR.

Thin PMMA films were prepared by spin coating of a solution of the polymer in toluene (concentration approximately 10 mg/mL) on a glass substrate. The single films were characterized using X-ray reflectometry.[29] A second film from another glass substrate was floated off onto a water surface and picked up on the bottom film. The double layers were dried under vacuum at 60 °C for 12 h and again characterized by X-ray reflectometry and interference microscopy prior to their use in neutron reflection experiments.

Reflectivity Measurements. The interface between the two polymer layers was studied by neutron reflectometry. With this method, it is possible to determine the interface profile with subnanometer resolution.

The reflectivity of a material is caused by the gradient of the refractive index n,[30] which is given by

$$n = 1 - \frac{\lambda^2}{2\pi} Nb \tag{1}$$

with λ the wavelength of the neutron beam and Nb the scattering length density of the polymer. Since the scattering lengths of hydrogen and deuterium are quite different,[31] a good contrast between protonated and deuterated polymers is achieved.

The reflectivity measurements were performed with the neutron reflectometer CRISP at the ISIS pulsed neutron source. The instrument is described elsewhere,[32] and only some relevant experimental details will be given here. A polychromatic pulsed neutron beam hits the sample at a fixed angle θ and is reflected into a detector which can be a ^{3}He single detector or a position sensitive detector. The neutron wavelength is determined by time of flight. For a first series of measurements (sample A) only incident wavelengths from 0.5 to 6.5 Å could be used. Experiments were performed with an incident angle θ = 0.45°. The intensity of the reflected neutrons was measured with a single ^{3}He gas detector. For a second series (sample B) a position sensitive detector could be used. The wavelength range 0.5−13 Å of the incident beam was available, and an incident angle of 0.83° was used. The broader wavelength spectrum of the incident beam gave a higher accuracy of the reflectivities, since a larger range of the incident wavevector perpendicular to the sample surface, k, could be measured.

The data were analyzed with a model fitting procedure. The profile is described by a layer model for the refractive model. The parameters of the model (refractive indices of the materials, layer thicknesses, and parameters characterizing the interfaces) are optimized using a grid search algorithm minimizing the deviations between experiment and fit characterized by the sum of the absolute deviations between experimental and calculated reflectivities divided by the experimental errors. For the calculation of the reflectivities from the model profile a matrix algorithm described by Lekner[30] is employed. The profile is approximated by a series of small steps. Each of these steps represents a homogeneous layer and is characterized by a 2 × 2 matrix. From the matrix characterizing the entire profile, which is obtained by multiplication of all the matrices, one can calculate the reflectivity of the layer system. In order to check whether the description of the data could be improved significantly by using different models, also model independent fit procedures were employed.[33]

Table 2. Annealing Times and Results of the Fits of the Neutron Reflection Measurements for the Interdiffusion of PMMAh/d M_w = 85 000 Sample A

measurement	additional annealing time relative to the previous measurement (min)	T (°C)	total annealing time (T_{ref} = 130 °C) (min)
A0			0.0
A1	30	124.3	2.25
A2	60	127.9	26.8
A3	60	136.1	605
A4	60	149.7	25907

	parameters polymer−polymer interface			thicknesses (nm)		
measurement	σ_2 (nm)	σ'_2 (nm)	P	d_{PMMA}	d_{PMMAd}	total interface width σ (nm)
A0	1.47			92.2	55.4	1.47 ± 0.2
A1	2.70			89.8	54.7	2.70 ± 0.3
A2	2.78			90.0	54.8	2.78 ± 0.3
A3	2.00	4.60	0.72	90.0	55.0	4.35 ± 0.4
A4	12.0			89.9	54.8	12.0 ± 1.5

Annealing Procedure. Samples A and B were subsequently annealed for varying times under vacuum at temperatures above the glass transition temperature in order to allow interdiffusion across the interface. Then samples were suddenly quenched to room temperature and measured with neutron reflectometry at room temperature. Since the diffusion time range covers several decades, the annealing was done at different temperatures. Annealing times at different temperatures were reduced to the reference temperature of 130 °C using the WLF equation[34]

$$\log a_T = c_1^0(T - T_0)/(c_2^0 + T - T_0) \tag{2}$$

with T the actual temperature and T_0 the reference temperature. The two constants c_1^0 and c_2^0 are characteristic for the polymer used. WLF parameters in the literature for PMMA differ due to different tacticities. For the PMMA's used in the study, the relatively high glass transition temperature is due to the predominantly atactic structure. Dynamic mechanical measurements were performed with the protonated polymer used. WLF parameters were determined from measurements of the shear moduli $G'(\omega)$ and $G''(\omega)$ at different temperatures in a frequency range between 0.1 and 100 rad/s using standard procedures.[35] Values of c_1^0 = 10.42 and c_2^0 = 58.5 K were obtained at a reference temperature of 130 °C. The annealing time at the temperature T is divided by a_T in order to obtain the reduced annealing time at the reference temperature T_0. Actual and reduced parameters of the annealing procedure are given in Tables 2 and 3. This procedure might give rise to uncertainties, since it is not clear whether the WLF equation with the parameters as determined above for the temperature dependence of the main chain motion holds for small diffusion paths. On small length scales, there might also be local motions involved. On the other hand the diffusion paths investigated are greater than the length scale of those local motions. Furthermore, the range of the annealing temperatures is small, so that deviations should not be significant. This is supported by the results of the two samples, which were

Table 3. Annealing Times and Results of the Fits of the Neutron Reflection Measurements for the Interdiffusion of PMMAh/d Sample B

measurement	additional annealing time relative to the previous measurement	T (°C)	total annealing time (T_{ref} = 130 °C) (min)
B0			0.0
B1	29	132.3	71
B2	50	132.3	197
B3	73	132.4	385
B4	50	135.5	779
B5	60	137.0	1564
B6	64	138.6	2944
B7	62	141.8	6408
B8	74	143.9	13815
B9	50	148.1	28221

	parameters polymer−polymer interface			thicknesses (nm)		
measurement	σ_2 (nm)	σ'_2 (nm)	P	d_{PMMAd}	d_{PMMA}	total interface width σ (nm)
B0	1.58			76.30	62.95	1.58 ± 0.2
B1	2.38			75.80	62.30	2.38 ± 0.2
B2	2.00	4.50	0.32	75.85	62.35	3.22 ± 0.3
B3	2.00	4.30	0.55	75.75	62.35	3.73 ± 0.3
B4	2.00	4.80	0.64	75.80	62.30	4.30 ± 0.4
B5	2.00	5.70	0.68	75.75	62.30	5.07 ± 0.4
B6	5.40			75.80	61.00	5.40 ± 0.4
B7	6.80			75.80	62.25	6.80 ± 0.6
B8	8.60			75.80	62.15	8.60 ± 0.7
B9	13.0			75.80	62.75	13.0 ± 1.3

annealed differently but gave the same values for the interface broadening with diffusion time.

Results and Discussion

A first series of measurements (sample A) were performed in order to get information about the time scale of interest. In a second series (sample B) smaller time intervals between successive annealings were chosen. The annealing times and the results of the fits to neutron reflectivity measurements are summarized in Tables 2 and 3. Typical neutron reflectivity curves are shown in Figure 1. The upper curve represents the unannealed sample. The interface between the two polymer layers is sharp and the Kiessig interference fringes are determined mostly by the deuterated polymer layer. With further annealing, the interface between the two polymer layers broadens and a change of the reflectivity curve first predominantly occurs at higher k values. Finally, with further broadening of the interface between the two polymer layers, the form of the reflectivity curve is significantly determined by the air−polymer and the polymer−glass interfaces. For the model fits, the refractive indices (for wavelength λ = 0.43 nm) $n_{PMMAh} = (1-3.10) \times 10^{-6}$, $n_{PMMAd} = (1-20.65) \times 10^{-6}$, and $n_{glass} = (1-9.50) \times 10^{-6}$ were used. The air−polymer interface could be described in good approximation by a simple error function with σ = 1.4 nm (sample A) and σ = 1 nm (sample B). This roughness of the sample surface did not change during annealing (within ±0.2 nm). In contrast to earlier investigations on the interdiffusion between PMMA and PVC,[13] a different sort of glass substrate was used in this work and the interface to the glass could be described by a simple error function with σ = 1.0 nm (sample A) and σ = 1.15 nm (sample B).

While for very short annealing times (less than approximately 100 min, measurements A0−A2 and B0−B1 according to Tables 2 and 3) and long annealing times (more than approximately 1600 min) the interface between the two polymer layers could be described by a single error function, this was not the case for intermediate annealing times. Instead of the simple error function, a more complicated profile for the refractive index had to be used

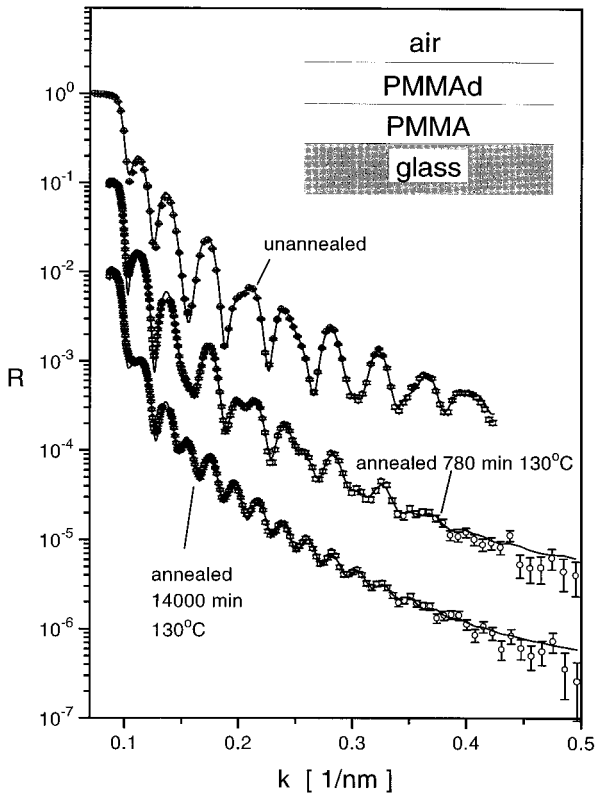

Figure 1. Measured neutron reflectivities versus k, the component of the incident wave vector perpendicular to the sample surface, at different annealing times (sample B). The solid lines show the best fits to the experimental data as explained in the text.

$$n(z') = n_1 + (n_2 - n_1)\frac{1}{\sqrt{2\pi}\sigma_2}\int_{-\infty}^{\infty}\tilde{\phi}(\eta)\exp\left(\frac{(z'-\eta)^2}{2\sigma_2^2}\right)d\eta \quad (3)$$

$$\text{and} \qquad \tilde{\phi}(z') = P\left(1 - \frac{1}{2}\,\mathrm{erfc}\left(\frac{z'}{\sqrt{2}\sigma'_2}\right)\right), \qquad z' < 0 \quad (4)$$

$$\tilde{\phi}(z') = 1 - \frac{P}{2}\,\mathrm{erfc}\left(\frac{z'}{\sqrt{2}\sigma'_2}\right), \qquad z' > 0 \quad (5)$$

$$0 \le P \le 1$$

with the refractive indices n_1 and n_2 of the two polymer layers (calculated values for protonated and deuterated PMMA) and z' as a coordinate perpendicular to the interface between the two polymer layers. Equations 4 and 5 describe a profile with a discontinuity of height $1 - P$ at the interface. This is convoluted with a Gaussian of width σ_2. Different values of σ_2 were used. The best fits could be obtained with σ_2 = 2 nm. The form of the interface between the two polymer layers is shown in Figure 2. In the upper part of the figure, the profile according to eqs 4 and 5 is shown. The resulting profile after the convolution, eq 3, is shown in the lower part of the figure. With increasing annealing time, one finds an increase of width σ'_2 and a decrease in the step

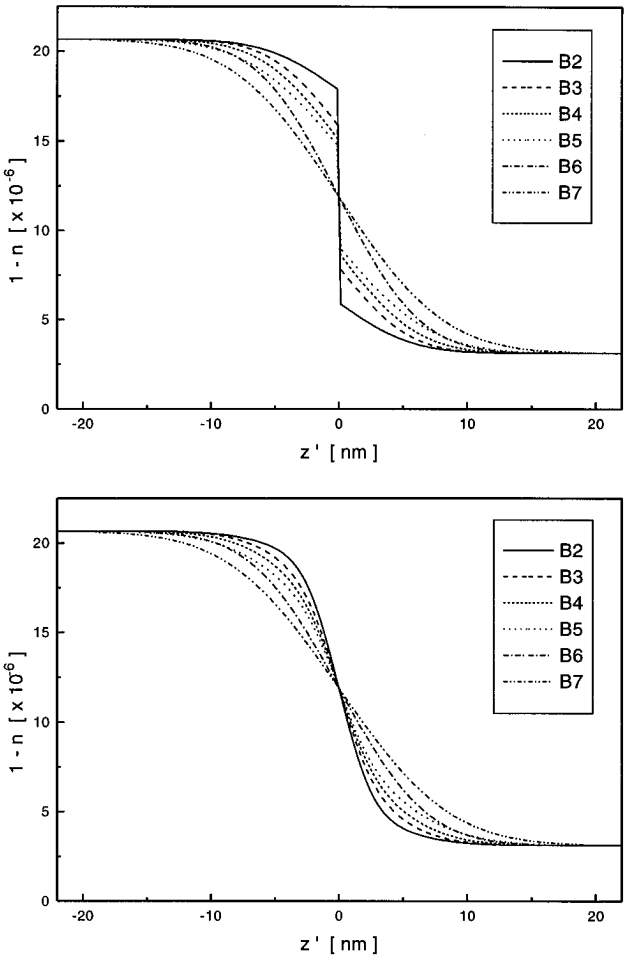

Figure 2. Refractive index profiles of the interface between PMMAd and PMMAh. $1 - n$ (for $\lambda = 0.43$ nm) is plotted versus the distance from the interface. The profiles used for the model calculations are shown in the lower part. They are obtained by a convolution of Gaussian of width $\sigma_2 = 2$ nm with the profiles of the upper part of the figure. With increasing annealing time the discontinuity at $z' = 0$ disappears and the width becomes larger. The samples notions correspond to different annealing times (see Table 3).

height expressed by the parameter P. Finally, the profile can be described by a simple error function, which corresponds to $P = 1$; i.e. the discontinuity disappears.

As mentioned above, this form of the profile can be understood in the framework of the reptation model.[4] If one considers only the reptative motion of the polymer chains, a profile with a discontinuity at the interface is expected. This discontinuity is smeared out because of the segmental motion.[28] Such a profile thus is consistent with the experiments. According to the reptation predictions,[3,4] the profile broadens and the discontinuity decreases with increasing annealing times, as mentioned before (see Figure 3, upper part). Approximately at the reptation time τ_d (for the calculation of the characteristic times, see below), the discontinuity disappears, which is also predicted. In the profile used for the modeling of the experimental data, this discontinuity is smeared out because of the free motion of the polymer segments within the tube of the reptation model[8,28] (see Figure 3, lower part).

The most dominant result from the fits is the increase of the interface width with time. To detain a simple parameter for the interface width, one can use as a measure of the width of the sophisticated profile defined

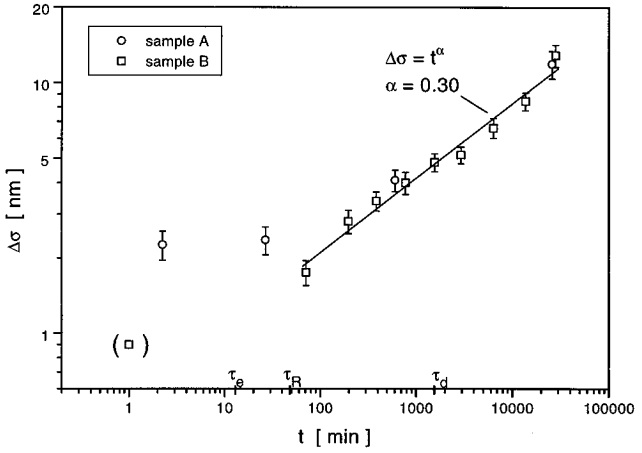

Figure 3. Double logarithmic plot of the interface broadening $\Delta\sigma$ versus annealing time (reduced to the reference temperature 130 °C). The data point in brackets indicates the unannealed sample. Also indicated are characteristic times according to the reptation model as explained in the text. The solid line is obtained from a fit of a straight line to the experimental data for annealing times longer than 30 min.

in eqs 3−5 the square root of the second moment of the derivative. In the case of a simple error function this is equivalent to the variance σ. Since the interface before annealing is not perfectly flat, one can correct the experimentally determined interface widths σ_{exp} for the initial roughness σ_o. The broadening of the interface is given by

$$\Delta\sigma = \sqrt{{\sigma_{exp}}^2 - {\sigma_o}^2} \tag{6}$$

$\Delta\sigma$ can be taken as the broadening of the interface due to segmental diffusion provided that the initial interface roughness does not change. The value of $\Delta\sigma$ is plotted versus the annealing time t in a double logarithmic scale in Figure 3. One can see that there is a sudden jump of the interface width after the very first annealing (this is indicated by the difference between the first data point and the data point in brackets, which should symbolize the width of the unannealed sample σ_o). After this initial jump $\Delta\sigma$ stays almost constant for some time. In a third regime at still later times the interface width increases as

$$\Delta\sigma \sim t^{\alpha}, \qquad \alpha = 0.30 \tag{7}$$

In order to compare these results with the reptation model, the knowledge of characteristic time and length scales is required. The reptation time τ_d is given by[15]

$$\tau_d = \frac{2{R_g}^2}{\pi^2 D_{Rept}} \tag{8}$$

One can calculate τ_d from the knowledge of the radius of gyration R_g and the self-diffusion coefficient D_{Rept}. For PMMA the radius of gyration has been measured and can be calculated[36]

$$\frac{R_g}{{M_w}^{1/2}} = 0.031 \frac{\text{nm}\cdot\text{mol}^{1/2}}{\text{g}^{1/2}}$$

For the protonated PMMA used, the diffusion coefficient was measured by X-ray reflectivity with a gold marker technique[37] at 145 °C. Using the WLF equation the

diffusion coefficient at 130 °C can be estimated. One obtains

$$\tau_d = 1547 \text{ min} \quad \text{for} \quad M_w = 85\,500 \quad \text{and} \quad T = 130 \text{ °C}$$

Since $\tau_R = \tau_d(3Z)$ and $\tau_e \simeq \pi^2\tau_d/(Z^3)$ with $Z = 5M_w/4M_e$, it is possible to calculate the Rouse relaxation time τ_R and the entanglement time τ_e. The molecular weight between entanglement is known from mechanical measurements: $M_e = 10\,000$.[38] One gets

$$\tau_R = 48 \text{ min} \quad \text{for} \quad M_w = 85\,500$$

and

$$\tau_e \simeq 13 \text{ min}$$

Values are noted in Figure 3.

Knowing the time regimes, one can compare the time dependence of the interface broadening $\Delta\sigma$ to the predictions of the reptation model for the mean square displacement of a chain segment $\langle r^2\rangle$ in the bulk[15]

$$\Delta\sigma(t) = \sqrt{\langle r^2\rangle/3} \tag{9}$$

The factor $^1/_3$ arises from the fact that with the reflectivity technique one can only see the movement of molecules in one dimension. According to the reptation model, as mentioned above, one expects for small times ($t \lesssim \tau_e$) $\Delta\sigma \sim t^{1/4}$. For $\tau_e \lesssim t \lesssim \tau_R$ $\Delta\sigma$ should behave like $t^{1/8}$. Between Rouse and reptation time $\tau_R \lesssim t \lesssim \tau_d$ one expects $\Delta\sigma \sim t^{1/4}$, and finally, Fickian diffusion should occur, $\Delta\sigma \sim t^{1/2}$, for $t \gtrsim \tau_d$. Using predictions of the reptation model in the bulk within the different time regimes,[15] one expects the following mean square displacements or diffusion paths at the characteristic times for the polymer used, $\Delta\sigma(t{=}\tau_e) = 3.9$ nm, $\Delta\sigma(t{=}\tau_R) = 3.9{-}4.7$ nm, and $\Delta\sigma(t{=}\tau_d) = 5.8{-}7.2$ nm.

Experimentally, three different time regimes can be clearly distinguished. After the very first annealing, a jump of the interfacial width is observed. A sudden relaxation of the chain segments with a time behavior, which cannot be resolved in detail, takes place. Within the reptation model, one might identify this regime with the free Rouse-type motion of the chain segments within the tube. Following this fast jump the interface width stays almost constant. This regime might be identified with the $t^{1/8}$ regime predicted from reptation theory. Finally, beginning approximately with the Rouse relaxation time τ_R, the interface broadening $\Delta\sigma$ increases according to $\Delta\sigma \sim t^{0.3}$, which corresponds reasonably well with the expected $t^{1/4}$ behavior. The transition to normal Fickian diffusion cannot be observed, which may be caused by the limitation of the neutron reflectivity technique when interface widths are larger than 15 nm. Of course there can be no doubt that for even longer times Fickian diffusion occurs. This has been confirmed by gold marker experiments[37] performed with PMMA of different molecular weights using also the protonated polymer employed in this work. The gold marker experiments show that the diffusion for longer times can be described by a diffusion coefficient with a molecular weight dependence $D \sim M^{-2}$, as predicted by the reptation model. However, the gold marker technique does not give information on the interface width directly. Other techniques with a better resolution like nuclear reaction analysis (NRA)[39] or secondary ion mass spectrometry (SIMS)[40] may be applied in this regime, but these techniques cause radiation damage in the case of PMMA.[41]

Even if the time regimes found are in qualitatively good accordance with the reptation model, there is no quantitative agreement. For instance, the broadening after the first annealing is approximately 2 nm instead of 4 nm, as expected. However, this might be caused by the inaccurate knowledge of the entanglement molecular weight M_e and its relation to the tube diameter. We also do not find the $t^{1/8}$ increase of the interface width although this might be difficult to determine within the scattering of points. A possible reason for the deviations between theory and experiment[29] is the initially distorted conformation of polymer chains at a surface, which is expected to differ significantly from the bulk. Computer simulations[42−45] indicate that the polymer chains are oriented near the surface. Chains are flattened in a direction parallel to the surface and one also expects an enrichment of chain ends at the surface. These effects will change the time behavior for small interdiffusion times. The distorted chain conformation will relax, and also the enrichment of chain ends will change the time behavior of the interdiffusion process.[4] Furthermore, the small interaction between protonated and deuterated PMMA chains[46] might also influence the interdiffusion process at early stages. However, all these effects are difficult to treat theoretically and are not investigated experimentally.

In addition there might be an effect of the sample preparation on the results obtained. This is shown by Sauer and Walsh,[47] who studied the time dependence of interdiffusion between poly(vinyl methyl ether) (PVME) with a glass transition temperature T_g of −31 °C and polystyrene (PS, $T_g \sim 105$ °C) at an annealing temperature below the glass transition temperature of polystyrene. They found that the conformation of the molecules in the as spun films is distorted, so that the diffusion at short times occurred much faster. By preannealing the PS film above T_g, this effect of the sample preparation could be eliminated. Since in our case the single films could not be preannealed, one might suppose that our results are strongly affected by the sample preparation. However, in contrast to Sauer and Walsh in our work the films were allowed to interdiffuse above the glass transition temperature of PMMA, and from their results (with a polystyrene film of similar molecular weight) it can be estimated that the sample preparation should play a role only at very small interdiffusion times. However, there is no understanding of this effect, so that it is difficult to quantify.

One can conclude that the experimental results concerning the form of the interfacial profile as well as the different time regimes observed for the broadening of the interface between the two polymer layers are in good qualitative agreement with the predictions of the reptation model. However, it is not possible to "proof" the reptation model because of the expected distortions of the initial chain conformation at the interface.

Similar experiments on the diffusion of polymers across an interface have been performed very systematically for polystyrene.[5−9,40,48] In these investigations mostly the neutron reflectivity technique is used because of its good resolution,[5−9] but for later stages of interdiffusion or for high molecular weights also other techniques like nuclear reaction analysis (NRA)[8] or

secondary ion mass spectrometry (SIMS)[40] are applied. Summing up those investigations, a quite similar time behavior of the interface broadening as in this work for PMMA is found: After the very first annealing, there is a jump of the interface width of approximately 2 nm. For intermediate times, there is only a slight increase of the interface width. For larger times the interface broadening behaves approximately as $\Delta\sigma \sim t^{1/4}$. At still larger times normal Fickian diffusion with $\Delta\sigma \sim t^{1/2}$ is observed using techniques like NRA[8] or SIMS.[40] It is also concluded that a simple error function is not always a good description for the polymer−polymer interface.[6,8] For instance, Reiter and Steiner[8] use a superposition of two error functions, which is similar to eqs 3−5, for the description of the polymer−polymer interface. For a relatively high molecular weight material ($M_w \approx$ 700 000), they find power laws for the time behavior of the different parameters describing the interfacial profile. Russell et al.[9,48] studied the interdiffusion between polystyrene with deuterated chain ends and polystyrene with a deuterated middle part of the chain. The interfacial profile during the diffusion process exhibits characteristic features, which can only be explained if one assumes that diffusion proceeds via the chain ends, as expected for the chain motion according to the reptation picture.

Conclusions

The initial stages of the diffusion of PMMA chains across an interface have been studied in detail using the neutron reflectivity technique. By the deuteration of one of the components, it is possible to investigate the broadening and the form of the concentration profile during interdiffusion with subnanometer resolution.

The broadening of the interface can be taken to be representative for the movement of chain segments across the initially quite sharp interface and thus gives some insight into chain dynamics in polymer melts. Several characteristic features are consistent with a picture given by the reptation model: Thus several time regimes of interfacial broadening are resolved with relatively sharp transitions at times, which at least qualitatively correspond to characteristic times of the reptation model. In particular, also the "reptation regime" with a power law exponent close to $^1/_8$ is observed. In addition, the form of the profile in an intermediate time regime is consistent with the reptation prediction that a jump should be present due to the particular movement of chains in the tube, which causes segmental movement across an interface mostly by chain ends. All those observations are thus consistent with predictions from the reptation model, while one, however, should keep in mind that deviations from this ideal behavior should be expected due to the initially distorted chain conformations, the enrichment of ends at the interface, and fluctuations due to capillary waves. Those effects are difficult to quantitize theoretically and experimentally and are therefore mostly neglected up to now.

The results of the diffusion experiments with PMMA thus yield similar conclusions, as they are observed with polystyrene. The particular behavior of chain segments at initial times of interdiffusion thus seems to be quite universal and characteristic for long chain molecules. A more rigorous test for reptation may be, however, still obtained with chains of different molecular weights or mobilities, and further experiments in this direction will be needed.

Acknowledgment. We acknowledge the help of Dr. J. Penfold, Dr. D. Bucknall (Rutherford Laboratories), Dr. H. Möbius, and B. Derichs during beam allocation at ISIS. We also thank A. Best and T. Hirschmann, who performed the dynamic mechanical measurements, and M. Bach for his technical assistence during X-ray characterization. This work was partially supported by the "Bundesministerium für Forschung und Technologie" (Grant 03-FI3MPG).

References and Notes

(1) Edwards, S. F. *Proc. Phys. Soc.* **1967**, *92*, 9.
(2) de Gennes, P. G. *J. Chem. Phys.* **1971**, *55*, 572.
(3) Brochard-Wyart, F.; de Gennes, P. G. *Makromol. Chem., Makromol. Symp.* **1990**, *40*, 167.
(4) de Gennes, P. G. In *Physics of Polymer Surfaces and Interfaces*; Sanchez, I. C., Ed.; Butterworth-Heinemann Publishers: Boston, 1992; p 55.
(5) Karim, A.; Mansour, A.; Felcher, G. P.; Russell, T. P. R. *Phys. Rev. B* **1990**, *42*, 6846.
(6) Felcher, G. P.; Karim, A.; Russell, T. P. *J. Non-Cryst. Solids* **1991**, *131−133*, 703.
(7) Stamm, M.; Hüttenbach, S.; Reiter, G.; Springer, T. *Europhys. Lett.* **1991**, *14*, 451.
(8) Reiter, G.; Steiner, U. *J. Phys. II* **1991**, *1*, 659.
(9) Agrawal, G.; Wool, R. P.; Dozier, W. D.; Felcher, G. P.; Russell, T. P.; Mays, J. W. *Macromolecules* **1994**, *27*, 4407.
(10) Fernandez, M. L.; Higgins, J. S.; Penfold, J. *Makromol. Chem. Macromol. Symp.* **1992**, *62*, 103.
(11) Sauer, B. S.; Walsh, D. J. *Macromolecules* **1991**, *24*, 5948.
(12) Guckenbiehl, B.; Stamm, M.; Springer, T. *Physica B* **1994**, *198*, 127.
(13) Kunz, K.; Stamm, M. *Makromol. Chem. Macromol. Symp.* **1994**, *78*, 105. Siqueira, D. F.; Schubert, D. W.; Erb, V.; Stamm, M.; Ameto, J. P. *Colloid Polym. Sci.* **1995**, *273*, 1041. Schubert, D. W.; Abetz, V.; Stamm, M.; Hack, T.; Siol, W. *Macromolecules* **1995**, *28*, 2519.
(14) Rouse, P. E. *J. Chem. Phys.* **1953**, *21*, 1272.
(15) Doi, M.; Edwards, S. F. *The Theory of Polymer Dynamics*; Clarendon Press: Oxford, U.K., 1986.
(16) Kremer, K.; Grest, G. S. *J. Chem. Phys.* **1990**, *92*, 5057.
(17) Paul, W.; Binder, K.; Heermann, D. W.; Kremer, K. *J. Chem. Phys.* **1991**, *95*, 7726.
(18) Kremer, K.; Grest, G. S. *J. Chem. Soc., Faraday Trans.* **1992**, *88*, 1707.
(19) Wittmer, J.; Paul, W.; Binder, K. *Macromolecules* **1992**, *25*, 7211.
(20) Richter, D.; Farago, B.; Fetters, L. J.; Huang, J. S.; Ewen, B.; Lartigue, C. *Phys. Rev. Lett.* **1990**, *64*, 1389.
(21) Butera, R.; Fetters, L. J.; Huang, J. S.; Richter, D.; Pyckout-Hintzen, W.; Zirkel, A.; Farago, B.; Ewen, B. *Phys. Rev. Lett.* **1991**, *66*, 2088.
(22) Richter, D.; Butera, R.; Fetters, L. J.; Huang, J. S.; Farago, B.; Ewen, B. *Macromolecules* **1992**, *25*, 2088.
(23) Richter, D.; Farago, B.; Butera, R.; Fetters, L. J.; Huang, J. S.; Ewen, B. *Macromolecules* **1993**, *26*, 795.
(24) Ewen, B.; Maschke, U.; Richter, D.; Farago, B. *Acta Polym.* **1994**, *45*, 795.
(25) Fleischer, G.; Fujara, F. *Macromolecules* **1992**, *25*, 4210.
(26) Tirrell, M.; Adolf, D.; Prager, S. *Springer Lecture Notes Appl. Math.* **1984**, *1063*, 37.
(27) Zhang, H.; Wool, R. P. *Macromolecules* **1989**, *22*, 3018.
(28) Zhang, H.; Wool, R. P. *Polym. Prepr. (Am. Chem. Soc., Div. Polym. Chem.)* **1990**, *31/2*, 511.
(29) Stamm, M. In *Physics of Polymer Surfaces and Interfaces*; Sanchez, I. C., Ed.; Butterworth-Heinemann Publishers: Boston, 1992; p 163. Stamm, M.; Schubert, D. W. *Annu. Rev. Mater. Sci.* **1995**, *25*, 325.
(30) Lekner, L. *Theory of Reflection*; Martinus Nijhoff Publishers: Amsterdam, 1987.
(31) Bacon, G. E. *Neutron Diffraction*, 3rd ed.; Clarendon Press: Oxford, U.K., 1979.
(32) Penfold, J.; Thomas, R. K. *J. Phys. Condens. Mater.* **1990**, *2*, 1369.
(33) Kunz, K.; Reiter, J.; Götzelmann, A.; Stamm, M. *Macromolecules* **1993**, *26*, 4316.
(34) Williams, M. L.; Landel, R. F.; Ferry, J. D. *J. Am. Chem. Soc.* **1955**, *77*, 3701.

(35) Ferry, J. D. *Viscoelastic Properties of Polymers*; John Wiley & Sons, Inc.: New York, 1980.
(36) Kirste, R. G.; Kruse, W. A.; Ibel, K. *Polymer* **1975**, *16*, 120.
(37) Liu, Y.; Reiter, G.; Kunz, K.; Stamm, M. *Macromolecules* **1993**, *26*, 2134.
(38) Masuda, T.; Kitagawa, K.; Onogi, S. *Polym. J.* **1970**, *1*, 418.
(39) Endisch, D.; Rauch, F.; Götzelmann, A.; Reiter, G.; Stamm, M. *Nucl. Instrum. Methods B* **1992**, *62*, 513.
(40) Whitlow, S. J.; Wool, R. P. *Macromolecules* **1991**, *24*, 5926.
(41) Tagawa, S. *Adv. Polym. Sci.* **1993**, *100*, 99.
(42) Madden, W. G. *J. Chem. Phys.* **1987**, *87*, 1405.
(43) Kumar, S. K.; Vacatello, M.; Yoon, D. Y. *J. Chem. Phys.* **1988**, *89*, 5206.
(44) Kumar, S. K.; Vacatello, M.; Yoon, D. Y. *Macromolecules* **1990**, *23*, 2189.
(45) Wang, J. S.; Binder, K. *Phys. I* **1991**, *1*, 1583.
(46) Hopkinson, I.; Kiff, F. T.; Richards, R. W.; King, S. M.; Munro, H. *Polymer* **1994**, *35*, 1722.
(47) Sauer, B. B.; Walsh, D. J. *Macromolecules* **1994**, *27*, 432.
(48) Russell, T. P.; Deline, V. R.; Dozier, W. D.; Felcher, G. P.; Agrawal, G.; Wool, R. P.; Mays, J. W. *Nature* **1993**, *365*, 235.

MA950187S